

A novel ultra-low temperature cofired $\text{Na}_2\text{BiZn}_2\text{V}_3\text{O}_{12}$ ceramic and its chemical compatibility with metal electrodes

Huaicheng Xiang¹ · Ying Tang¹ · Liang Fang¹ · Harshit Porwal³ · Chunchun Li^{1,2}

Received: 6 July 2016 / Accepted: 3 September 2016
© Springer Science+Business Media New York 2016

Abstract $\text{Na}_2\text{BiZn}_2\text{V}_3\text{O}_{12}$ ceramic was investigated as a promising microwave dielectric material for the ultra-low-temperature co-fired ceramic (ULTCC) technology. Dense $\text{Na}_2\text{BiZn}_2\text{V}_3\text{O}_{12}$ ceramic was prepared using the conventional solid-state method from 560 to 640 °C. X-ray diffraction data show that $\text{Na}_2\text{BiZn}_2\text{V}_3\text{O}_{12}$ ceramic crystallized into a cubic garnet structure with a space group $Ia\bar{3}d$. The sample sintered at 600 °C for 4 h has the highest relative density of 96.3 % and exhibits the optimum microwave properties with a relative permittivity of 22.3, a quality factor of 19,960 GHz (at 8.7 GHz), and a temperature coefficient of resonance frequency of +15.5 ppm/°C. The $\text{Na}_2\text{BiZn}_2\text{V}_3\text{O}_{12}$ ceramic was found to be chemically compatible with highly conductive aluminum and silver electrode. These results confirm that $\text{Na}_2\text{BiZn}_2\text{V}_3\text{O}_{12}$ ceramic can be a promising candidate for the ULTCC technology.

1 Introduction

To achieve the miniaturization and integration of the microwave components for wireless communication, low-temperature co-fired ceramic (LTCC) technology has become an important method that enables the fabrication of three-dimensional ceramic modules with a low dielectric loss and co-fired metal electrodes [1, 2]. For LTCC technology, a low sintering temperature lower than the melting point of metal electrodes (961 °C for Ag) is critical in addition to the appropriate relative permittivity (ϵ_r), a high quality factor ($Q \times f$), and a near-zero temperature coefficient of resonant frequency (τ_f) [3–5].

Recently, searching for novel microwave dielectric ceramics with intrinsic low firing temperatures, such as TeO_2 -based [6, 7], Bi_2O_3 -based [8, 9], and MoO_3 -based [10] systems, has attracted much attention. Some of them could co-fire with aluminum electrodes due to their ultra-low sintering temperatures <660 °C. The application of Al as the inner electrodes has accelerated the ultra-low-temperature co-fired ceramic (ULTCC) technology [10, 11]. More recently, several ULTCCs have been reported by the researchers, for example, BaTe_4O_9 ($\epsilon_r = 17.5$, $Q \times f = 54,700$ GHz, $\tau_f = -90$ ppm/°C and S. T. = 550 °C) [6], $\text{Bi}_2\text{Mo}_2\text{O}_9$ ($\epsilon_r = 38$, $Q \times f = 12,500$ GHz, $\tau_f = +31$ ppm/°C and S. T. = 620 °C) [10], and NaAgMoO_4 ($\epsilon_r = 7.9$, $Q \times f = 33,000$ GHz, $\tau_f = -120$ ppm/°C and S. T. = 400 °C) [12].

In our previous work [13, 14], some garnet vanadates were reported to have good microwave dielectric properties, such as $\text{LiCa}_3\text{ZnV}_3\text{O}_{12}$ ($\epsilon_r \sim 11.5$, $Q \times f \sim 81,100$ GHz, $\tau_f \sim -72$ ppm/°C, S. T. ~ 900 °C) and $\text{Na}_2\text{YMg}_2\text{V}_3\text{O}_{12}$ ($\epsilon_r \sim 12.3$, $Q \times f \sim 23,180$ GHz and $\tau_f \sim -4.1$ ppm/°C, S. T. ~ 850 °C). Most of them have chemical compatibility with silver electrode when sintered at their densification temperatures, making them possible candidates for

✉ Liang Fang
fanglianggl001@aliyun.com

✉ Chunchun Li
lichunchun2003@126.com

¹ State Key Laboratory Breeding Base of Nonferrous Metals and Specific Materials Processing, Guangxi Universities Key Laboratory of Non-ferrous Metal Oxide Electronic Functional Materials and Devices, College of Material Science and Engineering, Guilin University of Technology, Guilin 541004, China

² College of Information Science and Engineering, Guilin University of Technology, Guilin 541004, China

³ School of Engineering and Material Science, Queen Mary University of London, London E1 4NS, UK

LTCC applications. More recently, Zhou et al. [15] reported that $\text{Na}_2\text{BiMg}_2\text{V}_3\text{O}_{12}$ has an ultra-low sintering temperature $\sim 660^\circ\text{C}$ with a $\varepsilon_r \sim 23.2$, a $Q \times f \sim 3700$ GHz and a near-zero $\tau_f \sim +8.2$ ppm/ $^\circ\text{C}$. Therefore, it is worthwhile to investigate the $\text{Na}_2\text{BiMV}_3\text{O}_{12}$ ($M = \text{Zn}^{2+}$, Co^{2+} , Ni^{2+}) systems for an attempt to search for novel ultra-low-temperature co-fired ceramics.

In the present paper, an ultra-low-temperature co-fired ceramic $\text{Na}_2\text{BiZn}_2\text{V}_3\text{O}_{12}$ with garnet structure was reported. The sintering behavior, microstructure, microwave dielectric properties, and its chemical compatibility with both aluminum and silver were investigated in detail.

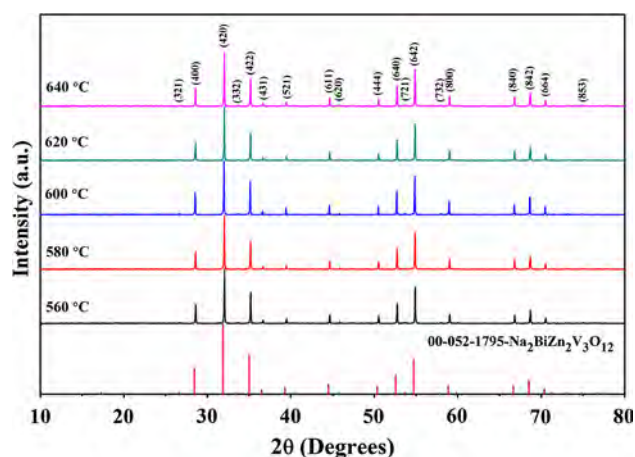


Fig. 1 X-ray diffraction patterns of $\text{Na}_2\text{BiZn}_2\text{V}_3\text{O}_{12}$ ceramics sintered at different temperatures from 560 to 640°C

2 Experimental procedure

$\text{Na}_2\text{BiZn}_2\text{V}_3\text{O}_{12}$ ceramic was prepared by the conventional solid-state reaction with high-purity oxides or carbonate powders, Na_2CO_3 (99 %, Guo-Yao Co. Ltd., Shanghai, China), Bi_2O_3 (99 %, West Long Chemical Co., Ltd., Guangdong, China), ZnO (99 %, Guo-Yao Co. Ltd., Shanghai, China), and NH_4VO_3 (>99 %, West Long Chemical Co., Ltd., Guangdong, China). Raw materials were weighed stoichiometrically and mixed, ball-milled in alcohol media for 6 h, followed by the calcination at 520°C for 4 h. The calcined powders were ball-milled for 6 h, dried, and pressed into cylinders with 12 mm in diameter and 7 mm in height under a pressure of 200 MPa. Polyvinyl alcohol (PVA) was added to the powders as binder. The samples were fired at 500°C for 2 h to burn-out the organic binder, and then sintered at 560 – 640°C for 4 h with a heating rate of $5^\circ\text{C}/\text{min}$. To investigate the chemical compatibility, $\text{Na}_2\text{BiZn}_2\text{V}_3\text{O}_{12}$ powders were mixed with 20 wt% aluminum and silver powders and co-fired at 640°C for 4 h.

X-ray diffraction (XRD) was employed to analyze the phase composition (1.54059 \AA , Model X'Pert PRO, PANalytical, Almelo, Holland) in the 2θ range of 10 – 80° . Bulk densities of the sintered samples were measured using Archimede's method. The microstructures were examined by scanning electron microscopy (SEM; FE-SEM, Model S4800, Hitachi, Japan). The microwave dielectric properties were analyzed using a network analyzer (Model

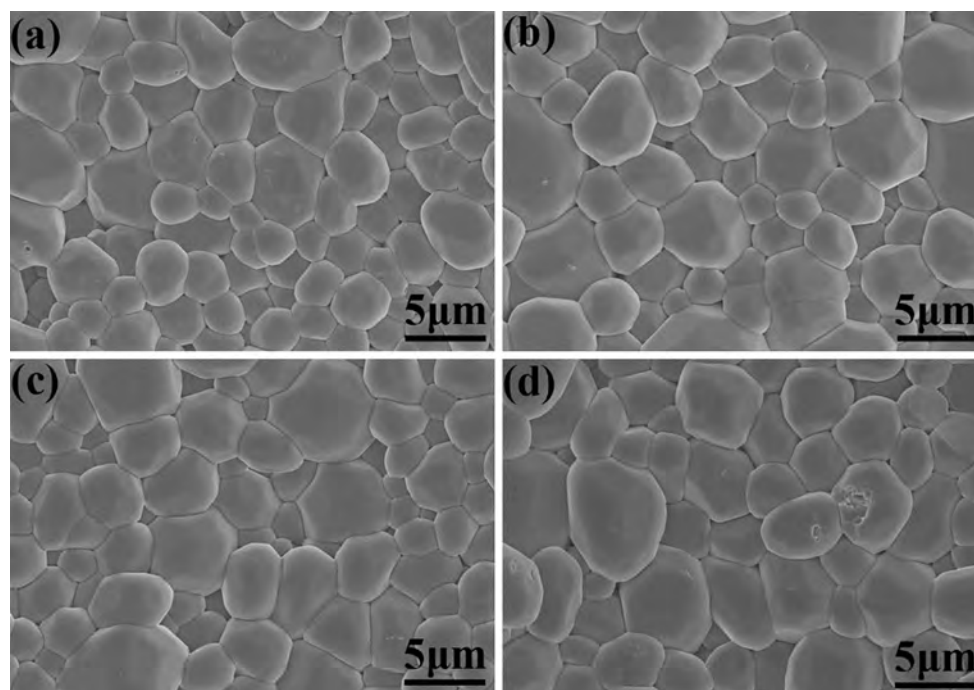


Fig. 2 SEM images of $\text{Na}_2\text{BiZn}_2\text{V}_3\text{O}_{12}$ ceramics sintered at **a** 560°C , **b** 580°C , **c** 600°C and **d** 620°C for 4 h in air

N5230A, Agilent Co., Palo Alto, California) and a temperature chamber (Delta 9039, Delta Design, San Diego, CA). The τ_f value was calculated using the following relationship:

$$\tau_f = \frac{f_{85} - f_{25}}{(85 - 25) \times f_{25}} \quad (1)$$

where, f_{85} and f_{25} are the resonant frequencies of the dielectric resonator at temperature 85 and 25 °C, respectively.

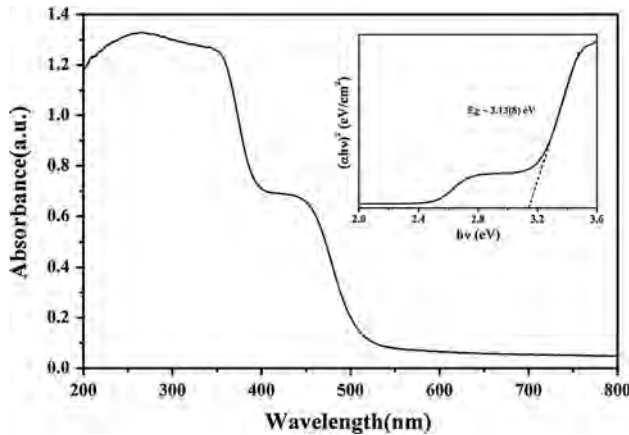
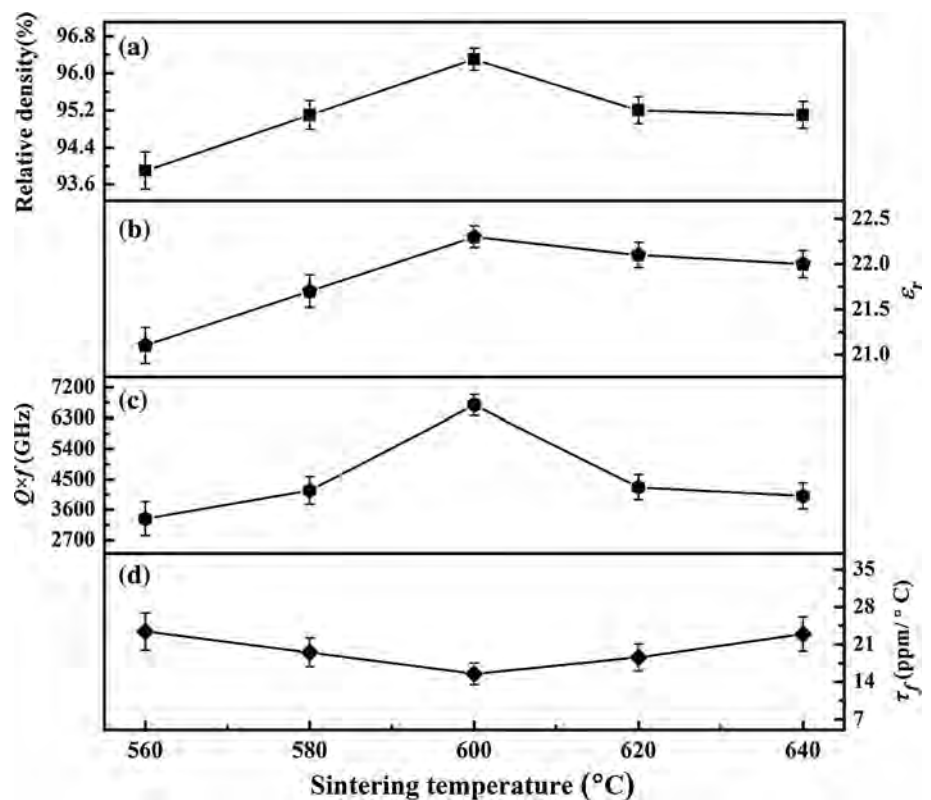


Fig. 3 UV-Vis light absorption spectrum of the $\text{Na}_2\text{BiZn}_2\text{V}_3\text{O}_{12}$. Inset plots of $(\alpha h\nu)^2$ versus energy $h\nu$ of $\text{Na}_2\text{BiZn}_2\text{V}_3\text{O}_{12}$ ceramic

Fig. 4 The relative densities (a) and microwave dielectric properties ϵ_r (b), $Q \times f$ (c), and τ_f (d) of $\text{Na}_2\text{BiZn}_2\text{V}_3\text{O}_{12}$ ceramics at different sintering temperatures



3 Results and discussions

Figure 1 shows the XRD patterns of the $\text{Na}_2\text{BiZn}_2\text{V}_3\text{O}_{12}$ ceramics sintered from 560 to 640 °C for 4 h. The observed peaks matched well with JCPDS card No. 52-1795 for $\text{Na}_2\text{BiZn}_2\text{V}_3\text{O}_{12}$ with no secondary phases detected, indicating the formation of pure-phase $\text{Na}_2\text{BiZn}_2\text{V}_3\text{O}_{12}$ with a cubic garnet structure.

SEM micrographs of $\text{Na}_2\text{BiZn}_2\text{V}_3\text{O}_{12}$ ceramics sintered at different temperatures are shown in Fig. 2. It shows that $\text{Na}_2\text{BiZn}_2\text{V}_3\text{O}_{12}$ ceramics could be well densified within the certain temperature range of 560–620 °C. The ceramics sintered at 560 °C showed a relatively porous microstructure (Fig. 2a) with small grains about 2–3 μm . With the increasing sintering temperature, the grain size increased along with a significant decrease in the porosity. A uniform and dense microstructure with closely packed grain morphology ($\sim 5 \mu\text{m}$ in average grain size) was obtained in the sample sintered at 600 °C. However, as the sintering temperature increased to 620 °C, abnormal grain growth and grain melting began to appear.

The optical absorption properties $\text{Na}_2\text{BiZn}_2\text{V}_3\text{O}_{12}$ ceramic were investigated by UV-Vis techniques. The values of the band gap energy (E_g) were calculated using following equation [16–18]:

$$(\alpha h\nu) = A(h\nu - E_g)^n \quad (2)$$

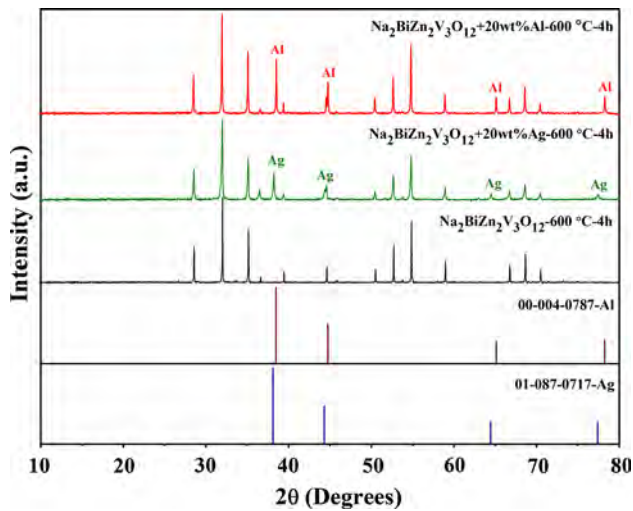


Fig. 5 X-ray diffraction patterns of $\text{Na}_2\text{BiZn}_2\text{V}_3\text{O}_{12}$ cofired ceramics with 20 wt% Al and 20 wt% Ag at 600 °C for 4 h

where A is a proportional constant, h is Planck's constant, ν is the frequency of vibration, E_g is the band gap energy, α is the absorption coefficient per unit length, and n is 0.5 and 2.0 for a direct transition semiconductor and indirect transition semiconductor, respectively [19–21]. The Ultraviolet–visible diffuse reflection spectra and plots of $(\alpha h\nu)^2$ versus energy $h\nu$ of $\text{Na}_2\text{BiZn}_2\text{V}_3\text{O}_{12}$ ceramic is displayed in Fig. 3. In the inset, the $\text{Na}_2\text{BiZn}_2\text{V}_3\text{O}_{12}$ sample shows a band gap energy of 3.13(8) eV.

Figure 4 shows the variations in relative densities and microwave dielectric properties of $\text{Na}_2\text{BiZn}_2\text{V}_3\text{O}_{12}$ ceramics as a function of the sintering temperature. The relative density showed a obvious dependence on the sintering temperature and a maximum value of 96.3 % (4.73 g/cm^3 of the theoretical density $\sim 4.91 \text{ g/cm}^3$) at 600 °C. As shown in Fig. 4b, ϵ_r increased from 21.1 to 22.3 as the sintering temperature increased from 560 to 600 °C,

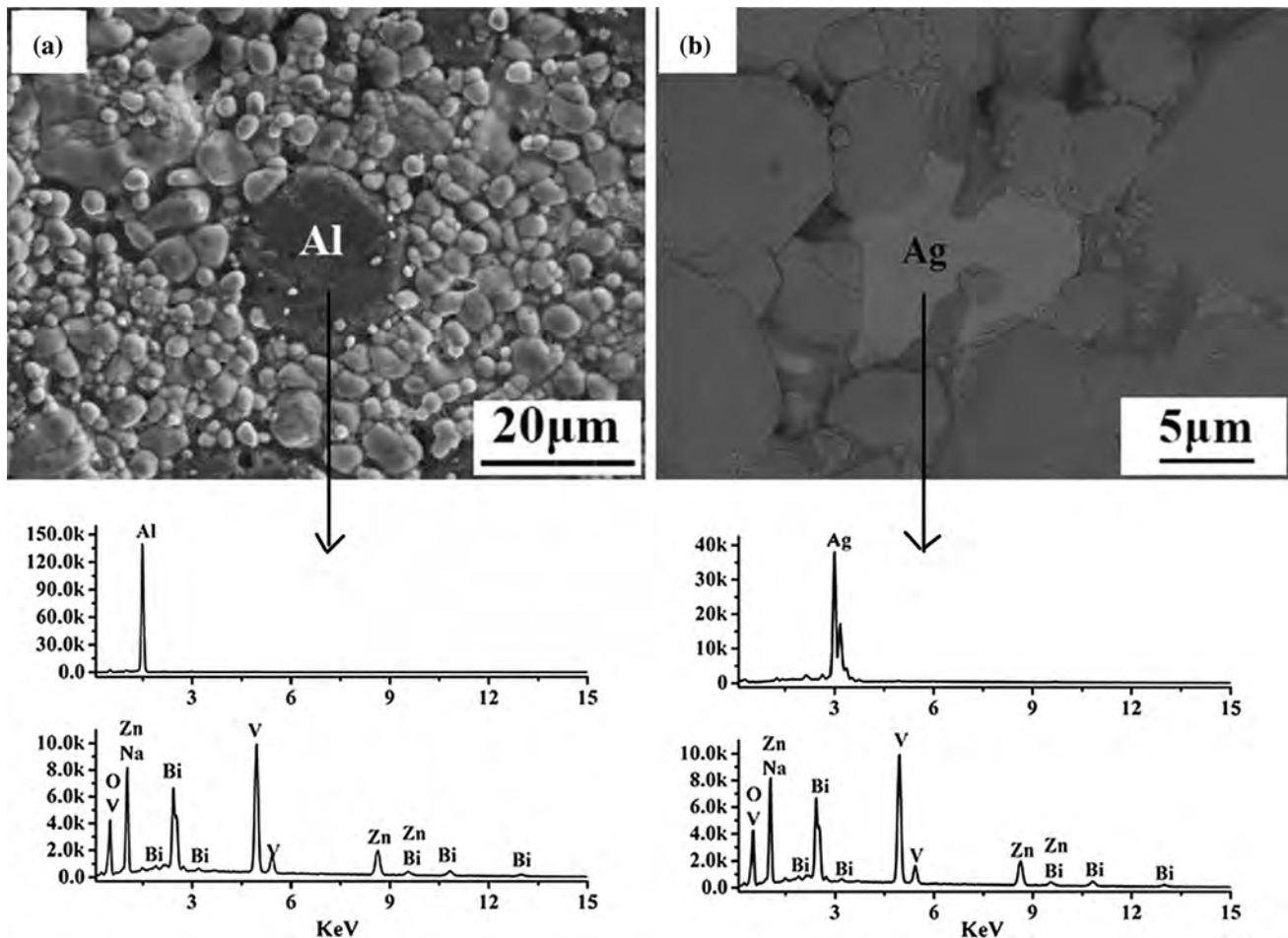


Fig. 6 Backscattered electron image micrograph and EDS analysis of the $\text{Na}_2\text{BiZn}_2\text{V}_3\text{O}_{12}$ ceramic with 20 wt% aluminum (a) and 20 wt% silver (b) sintered at 600 °C for 4 h

and then slightly decreased with further increasing temperature. The variation in ϵ_r with the increasing sintering temperature is consistent with that of the relative density. The lower permittivity at lower sintering temperature could be partly attributed to the existence of pores. The influence of the porosity on ϵ_r could be eliminated by applying Bosman and Having's correction [22, 23]:

$$\epsilon_{\text{corrected}} = \epsilon_m(1 + 1.5p) \quad (3)$$

where, p is the fractional porosity; $\epsilon_{\text{corrected}}$ and ϵ_m are the corrected and measured values of permittivity, respectively. The $\epsilon_{\text{corrected}}$ is about 23.5 for $\text{Na}_2\text{BiZn}_2\text{V}_3\text{O}_{12}$ sintered at 600 °C.

It is well known that there are many factors contributing to the dielectric loss at microwave region: the intrinsic factors and the extrinsic ones such as impurities, substitution, grain boundaries, grain morphology and shape, secondary phase, pores, dominate the $Q \times f$ value [24, 25]. As shown in Fig. 4c, an increase in $Q \times f$ value with sintering temperature was observed and a maximum value of 19,960 GHz was reached when sintered at 600 °C for 4 h. Thereafter, the $Q \times f$ value decreased, which might be due to extrinsic factors, such as the increase of pores and the abnormal grain growth. The τ_f values of $\text{Na}_2\text{BiZn}_2\text{V}_3\text{O}_{12}$ ceramics slightly fluctuated around +18 ppm/°C over the sintering range from 560 to 600 °C.

The XRD patterns of the cofired samples with 20 wt% aluminum and silver sintered at 600 °C are shown in Fig. 5 and XRD pattern of the pure $\text{Na}_2\text{BiZn}_2\text{V}_3\text{O}_{12}$ ceramic is also presented for comparison. For the cofired ceramic samples, only the peaks of $\text{Na}_2\text{BiZn}_2\text{V}_3\text{O}_{12}$ and the metals could be observed with no additional peaks detected. The backscattered electron image micrograph and EDS analysis of the cofired ceramics with 20 wt% aluminum (a) and silver (b) are shown in Fig. 6. The analysis revealed that the cofired ceramics were composed of both $\text{Na}_2\text{BiZn}_2\text{V}_3\text{O}_{12}$ grains and metal grains. These results confirm no chemical reaction between $\text{Na}_2\text{BiZn}_2\text{V}_3\text{O}_{12}$ and aluminum or silver when sintered at 600 °C for 4 h.

4 Conclusions

$\text{Na}_2\text{BiZn}_2\text{V}_3\text{O}_{12}$ ceramic can be prepared by conventional solid state reaction method and densified after sintering above 560 °C for 4 h in air. Optical absorption properties were investigated by UV–Vis techniques. The best microwave dielectric properties can be obtained in $\text{Na}_2\text{BiZn}_2\text{V}_3\text{O}_{12}$ ceramic sintered at 600 °C for 4 h, with a permittivity of 22.3, $Q \times f$ value of 19,960 GHz (at 8.7 GHz), and a positive τ_f value of +15.5 ppm/°C. From the XRD and EDS analysis, the $\text{Na}_2\text{BiZn}_2\text{V}_3\text{O}_{12}$ ceramic was found to be chemically compatible with aluminum or

silver powders at its sintering temperatures. Based on the experimental results of this research, $\text{Na}_2\text{BiZn}_2\text{V}_3\text{O}_{12}$ seems to be an attractive candidate for the ultra-low temperature co-fired ceramic technology.

Acknowledgments This research was supported by Natural Science Foundation of China (Nos. 21261007, 21561008, and 51502047), the Natural Science Foundation of Guangxi Zhuang Autonomous Region (Nos. 2015GXNSFBA139234, and 2015GXNSFFA139003), Project of Department of Science and Technology of Guangxi (No. 114122005-28), and Projects of Education Department of Guangxi Zhuang Autonomous Region (Nos. YB2014160, KY2015YB341, and KY2015YB122).

References

1. M.T. Sebastian, H. Jantunen, Low loss dielectric materials for LTCC applications: a review. *Int. Mater. Rev.* **53**, 57–90 (2008)
2. D. Zhou, C.A. Randall, H. Wang, L.X. Pang, X. Yao, Ultra-low firing high-k scheelite structures based on $[(\text{Li}_{0.5}\text{Bi}_{0.5})_x\text{Bi}_{1-x}][\text{MoV}_{1-x}\text{O}_4]$ microwave dielectric ceramics. *J. Am. Ceram. Soc.* **93**, 2147–2150 (2010)
3. L. Fang, Z.H. Wei, C.X. Su, F. Xiang, H. Zhang, Novel low-firing microwave dielectric ceramics: BaMV_2O_7 ($\text{M} = \text{Mg}, \text{Zn}$). *Ceram. Int.* **40**, 16835–16839 (2014)
4. T.W. Zhang, R.Z. Zuo, Effect of $\text{Li}_2\text{O}-\text{V}_2\text{O}_5$ addition on the sintering behavior and microwave dielectric properties of $\text{Li}_3(\text{Mg}_{1-x}\text{Zn}_x)_2\text{NbO}_6$ ceramics. *Ceram. Int.* **40**, 15677–15684 (2014)
5. A.K. Axelsson, N.M. Alford, Bismuth titanates candidates for high permittivity LTCC. *J. Eur. Ceram. Soc.* **26**, 1933–1936 (2006)
6. D.K. Kwon, M.T. Lanagan, T.R. Shrout, Microwave dielectric properties and low-temperature cofiring of BaTe_4O_9 with aluminum metal electrode. *J. Am. Ceram. Soc.* **88**, 3419–3422 (2005)
7. G. Subodh, M.T. Sebastian, Glass-free $\text{Zn}_2\text{Te}_3\text{O}_8$ microwave ceramic for LTCC applications. *J. Am. Ceram. Soc.* **90**, 2266–2268 (2007)
8. M. Valant, D. Suvorov, Processing and dielectric properties of sillenite compounds $\text{Bi}_{12}\text{MO}_{20-\delta}$ ($\text{M} = \text{Si}, \text{Ge}, \text{Ti}, \text{Pb}, \text{Mn}, \text{Bi}_{1/2}\text{P}_{1/2}$). *J. Am. Ceram. Soc.* **84**, 2900–2904 (2001)
9. D. Zhou, H. Wang, L.X. Pang, C.A. Randall, X. Yao, Bi_2O_3 – MoO_3 binary system: an alternative ultra low sintering temperature microwave dielectric. *J. Am. Ceram. Soc.* **92**, 2242–2246 (2009)
10. D. Zhou, C.A. Randall, A. Baker, H. Wang, L.X. Pang, X. Yao, Dielectric properties of an ultra-low-temperature cofiring $\text{Bi}_2\text{Mo}_2\text{O}_9$ multilayer. *J. Am. Ceram. Soc.* **93**, 1443–1446 (2010)
11. D. Zhou, L.X. Pang, H.D. Xie, J. Guo, B. He, Z.M. Qi, T. Shao, X. Yao, C.A. Randall, Crystal structure and microwave dielectric properties of an ultralow-temperature-fired $(\text{AgBi})_{0.5}\text{WO}_4$ Ceramic. *J. Inorg. Chem.* **2014**, 296–301 (2014)
12. D. Zhou, L.X. Pang, Z.M. Qi, J.B. Bing, X. Yao, Novel ultra-low temperature co-fired microwave dielectric ceramic at 400 degrees and its chemical compatibility with base metal. *Sci. Rep.* **4**, 5980 (2014)
13. C.X. Su, L. Fang, Z.H. Wei, X.J. Kuang, H. Zhang, $\text{LiCa}_3\text{ZnV}_3\text{O}_{12}$: a novel low-firing, high Q microwave dielectric ceramic. *Ceram. Int.* **40**, 5015–5018 (2014)
14. H.C. Xiang, L. Fang, X.W. Jiang, C.C. Li, Low-firing and microwave dielectric properties of $\text{Na}_2\text{YMg}_2\text{V}_3\text{O}_{12}$ ceramic. *Ceram. Int.* **42**, 3701–3705 (2016)

15. H.F. Zhou, Y.B. Miao, J. Chen, X.L. Chen, F. He, D.D. Ma, Sintering characteristic, crystal structure and microwave dielectric properties of a novel thermally stable ultra-low-firing $\text{Na}_2\text{BiMg}_2\text{V}_3\text{O}_{12}$ ceramic. *J. Mater. Sci.: Mater. Electron.* **25**, 2470–2474 (2014)
16. M.M. Momeni, Y. Ghayeb, Photoelectrochemical water splitting on chromium-doped titanium dioxide nanotube photoanodes prepared by single-step anodizing. *J. Alloys Compd.* **393**, 637–700 (2015)
17. M.M. Momeni, Y. Ghayeb, Photochemical deposition of platinum on titanium dioxide–tungsten trioxide nanocomposites: an efficient photocatalyst under visible light irradiation. *J. Mater. Sci. Mater. Electron.* **27**, 1062–1069 (2016)
18. M.M. Momeni, Y. Ghayeb, Preparation of cobalt coated TiO_2 and WO_3 – TiO_2 nanotube films via photo-assisted deposition with enhanced photocatalytic activity under visible light illumination. *Ceram. Int.* **42**, 7014–7022 (2016)
19. M.M. Momeni, Y. Ghayeb, Visible light-driven photoelectrochemical water splitting on ZnO – TiO_2 heterogeneous nanotube photoanodes. *J. Appl. Electrochem.* **45**, 557–566 (2015)
20. M.M. Momeni, Y. Ghayeb, Fabrication, characterization and photoelectrochemical behavior of Fe – TiO_2 nanotubes composite photoanodes for solar water splitting. *J. Electroanal. Chem.* **751**, 43–48 (2015)
21. M.M. Momeni, Y. Ghayeb, Z. Ghonchehi, Fabrication and characterization of copper doped TiO_2 nanotube arrays by in situ electrochemical method as efficient visible-light photocatalyst. *Ceram. Int.* **41**, 8735–8741 (2015)
22. E.S. Kim, B.S. Chun, R. Freer, R.J. Cernik, Effects of packing fraction and bond valence on microwave dielectric properties of $\text{A}^{2+}\text{B}^{6+}\text{O}_4$ (A^{2+} : Ca, Pb, Ba; B^{6+} : Mo, W) ceramics. *J. Eur. Ceram. Soc.* **30**, 1731–1736 (2010)
23. C.F. Tseng, Microwave dielectric properties of a new $\text{Cu}_{0.5}\text{Ti}_{0.5}\text{NbO}_4$ ceramics. *J. Eur. Ceram. Soc.* **35**, 383–387 (2015)
24. S. George, M.T. Sebastian, Synthesis and microwave dielectric properties of novel temperature stable high Q, $\text{Li}_2\text{ATi}_3\text{O}_8$ ($\text{A} = \text{Mg}, \text{Zn}$) ceramics. *J. Am. Ceram. Soc.* **93**, 2164–2166 (2010)
25. H.F. Zhou, X.B. Liu, X.L. Chen, L. Fang, Y.L. Wang, $\text{ZnLi}_{2/3}\text{Ti}_{4/3}\text{O}_4$: a new low loss spinel microwave dielectric ceramic. *J. Eur. Ceram. Soc.* **32**, 261–265 (2012)